

Fermi-Level Tuning of Topological Insulator Thin Films

Masaki Aitani¹, Yusuke Sakamoto¹, Toru Hirahara^{1*}, Manabu Yamada¹, Hidetoshi Miyazaki^{2†}, Masaharu Matsunami², Shin-ichi Kimura^{2‡}, and Shuji Hasegawa¹

¹Department of Physics, University of Tokyo, Bunkyo, Tokyo 113-0033, Japan

²UVSOR Facility, Institute for Molecular Science, Okazaki, Aichi 444-8585, Japan

E-mail: hirahara@surface.phys.s.u-tokyo.ac.jp

Received April 24, 2013; revised June 15, 2013; accepted July 17, 2013; published online October 16, 2013

Topological insulators are insulating materials but have metallic edge states with peculiar properties. They are considered to be promising for the development of future low energy consumption nano-electronic devices. However, there is a major problem: Naturally grown materials are not truly insulating owing to defects in their crystal structure. In the present study, we have examined the electronic structure and transport properties of topological insulator ultrathin Bi₂Te₃ films by angle-resolved photoemission spectroscopy and in situ transport measurements. To realize a truly bulk insulating film, we tried to tune the Fermi-level position using two methods. The first of these, i.e., changing the Si substrate temperature during film growth (350–450 K) to reduce the defects in the grown films, had some effect in reducing the bulk residual carriers, but we could not fabricate a film that showed only the surface states crossing the Fermi level. The second method we employed was to incorporate Pb atoms during film growth since Pb has one less electron than Bi. When the films were grown at around 350 K, we observed a systematic shift in the Fermi level and obtained a bulk insulating film, although it was not possible to move the Dirac point just at the Fermi level. The change in the measured film conductivity was consistent with the shift in the Fermi level and suggested the detection of the surface-state conductivity. For films grown at a higher substrate temperature (450 K), the Fermi level could be tuned only slightly and a bulk n-type film was obtained. Pb incorporation changes the shape of the Dirac cone, suggesting the formation of a stoichiometric ternary alloy of Bi, Pb, and Te, which is another topological insulator.

© 2013 The Japan Society of Applied Physics

1. Introduction

Topological insulators have attracted much attention from a wide variety of researchers in condensed matter physics as well as device physics for spintronics. They are mathematically characterized by the so-called Z_2 topological number.¹⁾ While the bulk is insulating, there is a metallic edge or surface state that is topologically protected and hence robust against weak perturbation or disorder. These surface states also have a spin-helical structure; i.e., the spin is locked with the momentum. Angle-resolved photoemission spectroscopy (ARPES) measurements have directly shown the presence of such surface states, and their spin structure has been resolved for a variety of materials.^{2–5)}

Owing to the spin-helical nature of their surface states, topological insulators can exhibit spin polarization by applying an electric field even in the absence of a magnetic field.⁶⁾ When doped with ferromagnets, a quantum anomalous Hall effect will arise that is also controllable by the electric field.⁷⁾ Moreover, it has been predicted that when topological insulators are placed into contact with superconductors, Majorana fermions will emerge.⁸⁾ Because of their non-Abelian nature, these Majorana fermions are said to be applicable in topological quantum computation.⁹⁾ Also, since typical examples such as Bi₂Te₃ and Bi₂Se₃ are known to be thermoelectric materials, topological insulators are expected to be utilized in high-performance thermoelectric devices.¹⁰⁾ All these unique properties make topological insulators promising candidates for fabricating high-speed, low-energy-consumption, next-generation, nano-scale electronic devices.

One critical issue in the study of topological insulators is the realization of a true bulk insulator. In principle, when a sample is cooled to low temperatures, the insulating bulk

carriers will freeze out, and thus only the metallic surface states should contribute to the physical properties. But it has been known that some unwanted doping occurs, and in reality, it is difficult to make the bulk “insulating”. ARPES studies have shown that naturally grown stoichiometric samples are actually n-type semiconductor owing to inevitable defects or substitutions in the lattice.^{2,11)} Many attempts have been made to perform the opposite doping with intentional substitution of atoms, and these have been partly successful.¹²⁾ Recently, two new materials, BiSbTeSe¹³⁾ or Sn-doped Bi₂Te₂Se¹⁴⁾ were shown to be bulk insulating crystals.

Another interesting question is how the surface states will be affected in ambient conditions. In ARPES, the experiments are all performed under ultrahigh vacuum conditions where the crystals are cleaved in situ prior to the measurement. In contrast, transport measurements are performed ex situ in air. Whether the same surface states are present in both environments is an open question. Some reports have focused on the oxidation of these materials.¹⁵⁾ There are actually some transport measurements that show that the surface states degrade due to oxidation.¹⁶⁾ Others claim that keeping the topological insulator crystals in air will just induce carrier doping.¹³⁾ In this respect, it is desirable to perform in situ transport measurements^{17,18)} that would be free of the complicating effect of oxidation.

In the present work, we have attempted to tune the Fermi-level (E_F) position of a Bi₂Te₃ film grown on Si(111). The advantage of using an ultrathin film is to enhance the surface/volume ratio by decreasing the sample thickness and making the surface-state transport dominant. However, if the film is too thin, there will be no topological surface states.¹⁹⁾ Therefore, we have fabricated three quintuple layer (1 QL = 10.2 Å) films and measured the band dispersion as well as performed in situ transport measurements. For the doping, we have employed two methods. The first of these is to change the substrate temperature during film growth and control the defect density. ARPES measurements showed that Fermi-

[†]Present address: Department of Environmental and Materials Engineering, Nagoya Institute of Technology, Nagoya 466-8555, Japan.

[‡]Present address: Graduate School of Frontier Biosciences, and Department of Physics, Osaka University, Suita, Osaka 565-0871, Japan.

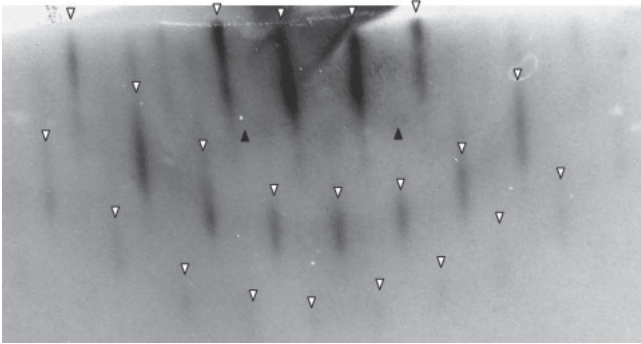


Fig. 1. RHEED pattern of a 3 QL Bi₂Te₃ film. Downward-pointing, white triangles indicate the 1 × 1 spots, while upward-pointing, black triangles indicate the Kikuchi lines.

level tuning was possible to some extent, but the doping was complicated. In situ transport measurements did not show systematic change with the band dispersion. As a second, alternative method, we have incorporated Pb into the Bi₂Te₃ film. We found that for rather low substrate temperatures during film growth (350 K), it was possible to realize a bulk insulator when 10% Pb was alloyed with Bi; ARPES showed that only the surface states crossed the Fermi level. In contrast, it was not possible to realize a bulk insulating state when the substrate temperature was high (450 K). In both cases, we found a change in the shape of the Dirac cone that suggested the formation of another stoichiometric alloy of Bi, Pb, and Te, which are also known as topological insulators. Furthermore, the measured film conductivity was in accordance with the change in the band dispersion. Thus, these films may enable the fabrication of devices utilizing the intriguing properties of topological surface states.

2. Experimental Methods

The ultrathin Bi₂Te₃ films were fabricated in situ by a method similar to that in Ref. 20. First, a clean Si(111)-7 × 7 surface was prepared on an n-type substrate (P-doped, 1–10 Ω·cm at room temperature) by a cycle of resistive heat treatments. Then Bi was deposited on the 7 × 7 structure at 350–450 K under Te-rich conditions. This procedure is reported to result in a smooth epitaxial film, as can be clearly seen in the RHEED pattern in Fig. 1, indicating the 1 × 1 periodicity of the Bi₂Te₃(111) surface as well as the Kikuchi lines. Scanning tunneling microscopy measurements have also confirmed the formation of high-quality films with an atomically flat surface.²¹ It is also known that the minimum film thickness that can be achieved by this method is a quintuple layer (1 QL = 10.2 Å), and the films grow in a QL-by-QL fashion as revealed by the RHEED intensity oscillation.²² For carrier doping, we have alloyed Pb with Bi and co-deposited them with fixed flux ratios under Te-rich conditions. This co-deposition also resulted in a smooth epitaxial film with no noticeable change in lattice constant as far as revealed by the RHEED pattern.

In situ conductivity measurements were performed with monolithic micro four-point probes (MFPP) in a custom-made UHV chamber¹⁷ at room temperature without applying a magnetic field. The conductivity of the underlying substrate Si(111)-7 × 7 is much smaller than the measured

values and can be neglected.²³ Furthermore, it is likely that the 7 × 7 structure is destroyed by the film formation. The vertical error bars in the conductivity measurements represent the data scattering caused by measuring different positions of the sample surface. Since the probe spacing (20 μm) is much smaller than the sample size (typically 2 × 10 mm²), such scattering reflects the inhomogeneity of the ultrathin films (nonuniform distribution of defects and steps, etc.). The scattering is not so large as can be seen in Figs. 3, 5, and 9, meaning that the films are rather homogeneous, which has also been confirmed by measuring the core-level photoemission spectra of Bi, Te, and Pb at various parts of the sample. The only exception is at the sample edge near the clamps where the underlying substrate is contaminated.

ARPES experiments were performed at BL-5U of UVSOR-II using an electron analyzer of MBS-Toyama A-1. The energy and angular resolutions were 20 meV and 0.2°, respectively. The photon energy used was $h\nu = 21$ eV and the measurements were done at 10 K. We emphasize that both the conductivity and ARPES measurements were conducted in situ under UHV conditions, ensuring that the same surface states were present in both measurements.

3. Results and Discussion

Experimentally, it is known that Bi₂Te₃ films can exhibit Dirac-like surface-state band dispersion from 2 QL. For the 1 QL film, the top and bottom surface Dirac cones interact, which results in a massive Dirac cone (parabolic band dispersion).²⁰ Theoretically, it has been pointed out that three or more QL films have topologically nontrivial surface states.²⁴ Therefore, in the following, we will discuss the band dispersion and film conductivity of a 3 QL Bi₂Te₃ film.

3.1 Substrate temperature dependence

First, we show how the band dispersion is affected by changing the substrate temperature during the growth of the Bi₂Te₃ films. Figure 2 shows the Fermi surface (top row) and the band dispersion (bottom row) of the 3 QL Bi₂Te₃ film when the substrate temperature (T_{Si}) during the growth is 350 (a), 421 (b), 431 (c), and 449 K (d). The outer hexagons and inner circles in the Fermi surface of Fig. 2(a) indicate the Dirac-cone surface state and bulk conduction band, respectively. For the other data, the distinction between the bulk and surface is rather unclear, but by analyzing the photoemission spectra in detail, we can outline the individual components and their probable schematic shape is shown in Figs. 2(b)–2(d). This indicates that all of the films are electron-doped (n-type), which means the bottom of the bulk conduction band is below E_F . The red line shows the position of the Dirac point (DP). It can be seen that the DP shifts towards E_F as T_{Si} is increased. This is basically consistent with the results of a previous study showing the Fermi-level tuning of a 60 QL Bi₂Te₃ film.²⁵ However, although they succeeded in changing the bulk carrier from electrons (n-type) to holes (p-type), Fig. 2(d) shows that the films remain n-type throughout the temperature range we have studied; the intensity at the center of the Fermi surface in Figs. 2(b)–2(d) means that the bulk conduction band remains below E_F .²⁶ Furthermore, we note that the energy positions of the surface and the bulk states shifted differently: While the surface states shifted by about 0.2 eV towards the Fermi level from (a) to (d), the bulk

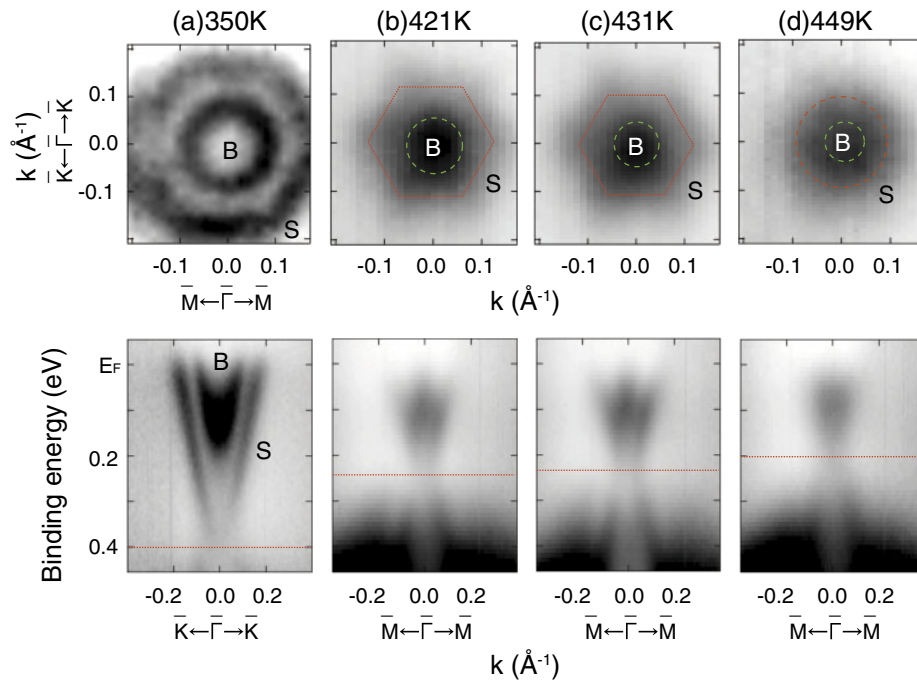


Fig. 2. (Color online) Fermi surface (top row) and the band dispersion around the $\bar{\Gamma}$ point (bottom row) of the 3 QL Bi_2Te_3 film when the substrate temperature (T_{Si}) during growth was 350 (a), 421 (b), 431 (c), and 449 K (d). The red line indicates the position of the Dirac point. B and S denote bulk and surface states, respectively, and the hexagons and circles indicate the shapes of the Fermi surface.

states appear to have shifted by less than 0.1 eV. The origin of this behavior is not clear, but this shows that the slight change in substrate temperature as well as film thickness can have a different influence on the surface and bulk band structure.

Figure 3(a) shows the change in the bulk and surface-state carrier density as a function of the substrate temperature derived from the area of the Fermi surface in Fig. 2. Figure 3(b) compares the change in DP energy position (red filled squares) with measured film two-dimensional (2D) conductivity (blue open diamonds). As discussed above, the DP shifts systematically towards E_F for higher T_{Si} . On the other hand, the 2D conductivity is $65 \mu\text{S}$ for the film grown at 350 K, and increases to $\sim 250 \mu\text{S}$ for films with $T_{\text{Si}} = 405\text{--}430 \text{ K}$, then returns to $80 \mu\text{S}$ for the film with $T_{\text{Si}} = 450 \text{ K}$. Thus, we conclude that there is no correspondence between the film conductivity and the Dirac point energy. This is not surprising since we showed that the energy shifts of the surface and bulk seem to be different. Furthermore, since conductivity is given by $\sigma = en\mu$, where n is carrier density and μ is mobility, conductivity is not only determined by n (the Fermi-level tuning). Since mobility is influenced by defect density, we need to know how the defect distribution varies with T_{Si} . Obtaining this information requires a detailed study using different experimental techniques.

In summary, we attempted to fabricate a truly bulk insulating 3 QL Bi_2Te_3 film by tuning the Fermi-level position through changing T_{Si} . The approach was, to some extent, successful; however, the bulk and surface states were affected differently. Furthermore, there was no clear relationship between the film conductivity and the E_F position. This suggests that changing T_{Si} is not enough to make a bulk insulating film.

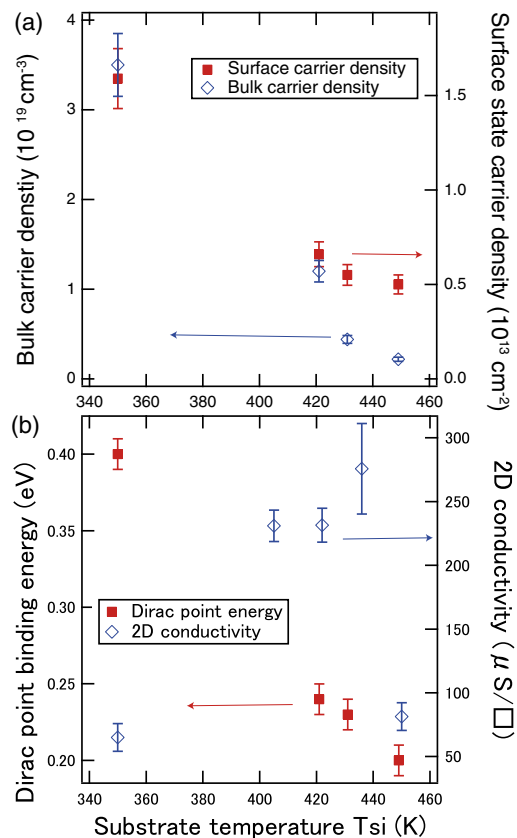


Fig. 3. (Color online) (a) Change of the bulk and surface-state carrier density for the 3 QL Bi_2Te_3 films formed at different substrate temperatures from the Fermi surface of Fig. 2. These values represent the values for zero kelvin. (b) Comparison of the change in the Dirac point position (from Fig. 2) with the measured film 2D conductivity.

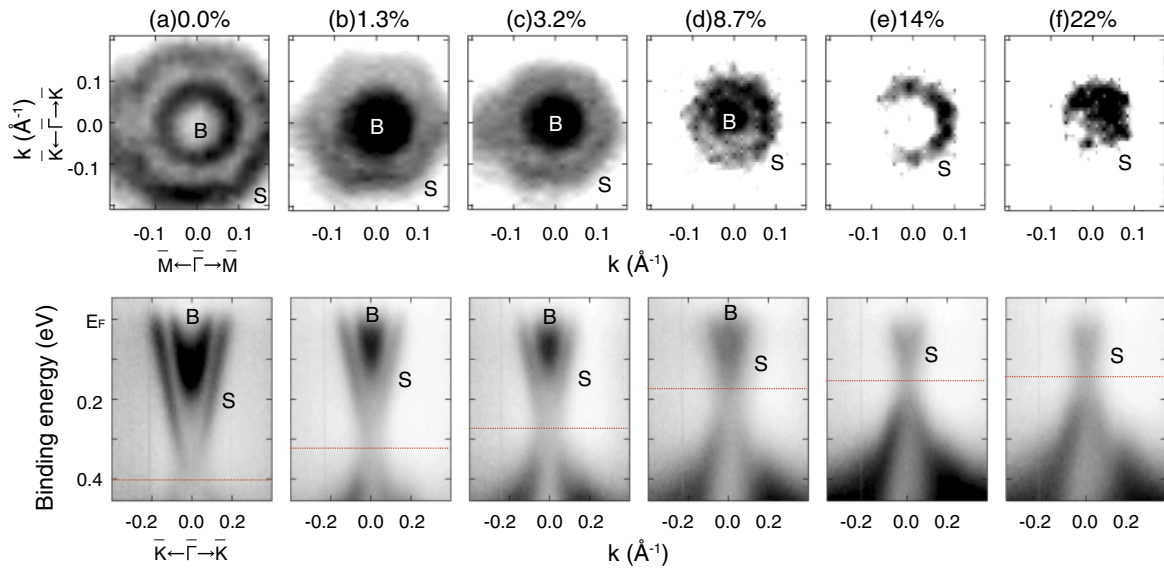


Fig. 4. (Color online) Fermi surface (top row) and band dispersion (bottom row) of the 3 QL Bi_2Te_3 film grown at $T_{\text{Si}} = 350$ K with a Pb concentration of 0 (a), 1.3 (b), 3.2 (c), 8.7 (d), 14 (e), and 22% (f). The red line indicates the position of the Dirac point. B and S represent the bulk and surface states, respectively.

3.2 Pb doping dependence: low T_{Si}

An alternative way to tune the Fermi level of Bi_2Te_3 films would be to replace Bi with Pb. Since Pb has one less electron than Bi, this would act as hole doping and decrease the bulk electron density. First, we show the results of the Pb doping effect when the Si temperature during growth is 350 K. Figure 4 shows the Fermi surface (top row) and the band dispersion (bottom row) of the 3 QL Bi_2Te_3 film when $T_{\text{Si}} = 350$ K with a Pb concentration of 0 (a), 1.3 (b), 3.2 (c), 8.7 (d), 14 (e), and 22% (f). For the undoped and 1.3–8.7% doped films [(a)–(d)], there are two (bulk and surface) Fermi surfaces. Their size shrinks gradually, and at 14% doping, the bulk Fermi surface seems to disappear; we can only recognize a single Fermi ring of the Dirac cone in (e). The features are more or less the same for the 22%-doped film in (f), though the Dirac-cone Fermi ring has shrunk. The DP position (red line) shifts systematically towards the Fermi level, but seems to saturate around 0.12 eV below E_{F} [(f)]. From the area of the Fermi surface, it is possible to estimate the carrier density, which is shown in Fig. 5(a). In contrast to the discussion in the previous section where the changes in the energy positions of the bulk and surface states were different, they seem to shift together in the present case. This can also be gleaned from the conductivity measurements. Figure 5(b) compares the measured film conductivity (blue open diamonds) to the shift in the Dirac point (red filled squares). The conductivity gradually decreases as Pb is doped from its initial value of $65 \mu\text{S}$ and saturates at around $20 \mu\text{S}$ for doping levels higher than $\sim 10\%$. We can say that there is a systematic relationship between the DP energy and the conductivity, unlike in the results shown in the previous section. Thus, the change in carrier concentration presumably corresponds to the change in conductivity. Since only the Dirac-cone surface state crosses the Fermi level with a Pb density of more than $\sim 10\%$, the saturated value of $20 \mu\text{S}$ likely corresponds to the surface state contribution, but further study is needed to draw a definite conclusion. As the measurements were

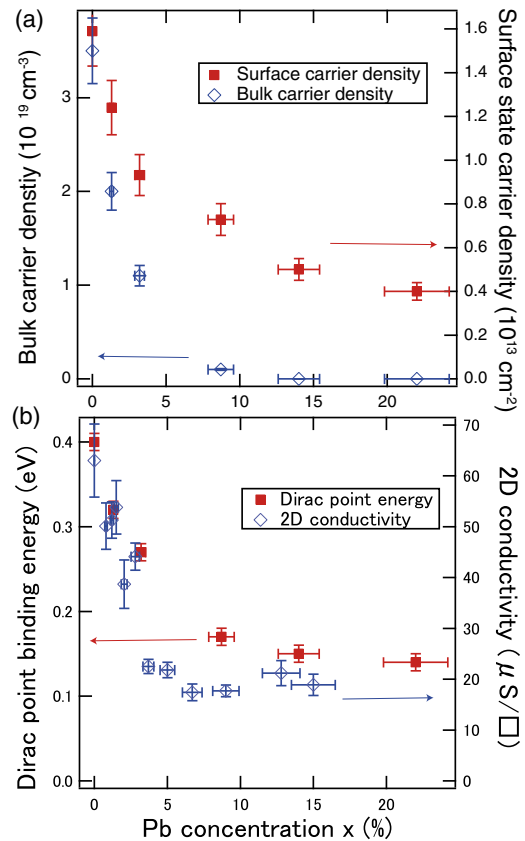


Fig. 5. (Color online) (a) Change in the bulk and surface-state carrier density for 3 QL Bi_2Te_3 films doped with different Pb concentrations from the Fermi surface of Fig. 4. These values represent the values at zero kelvin. (b) Comparison of the change in the Dirac point position (from Fig. 4) with the measured film 2D conductivity.

performed at room temperature, there should still be 10^{17} cm^{-3} bulk carriers present, considering the relatively small activation gap (0.15 eV for undoped Bi_2Te_3) for the bulk carriers. Since information concerning the mobility cannot

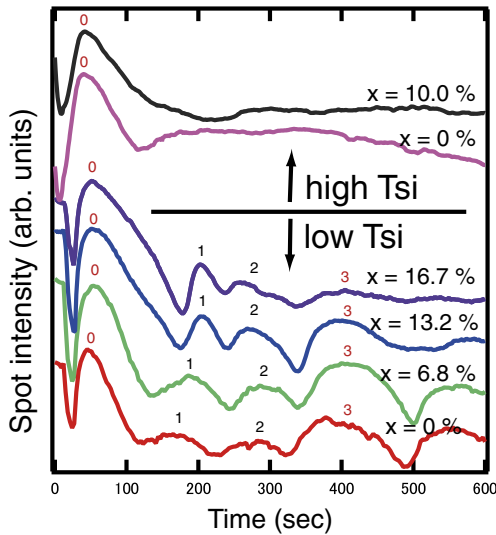


Fig. 6. (Color online) Specular RHEED spot intensity oscillation during film growth for varying Pb-doping concentration, x . Low T_{Si} corresponds to 350 K and high T_{Si} corresponds to 450 K.

be determined from the present measurement, we cannot distinguish the bulk and surface contributions. If we assume that only the surface state contributes to the measured conductivity, the mobility at room temperature can be estimated to be $22 \text{ cm}^2 \cdot \text{V}^{-1} \cdot \text{s}^{-1}$.

We have found that Pb does not actually donate one hole per atom. The ratio (induced hole carriers)/(incorporated Pb atoms) changes from 0.2 for the 1.3%-doped film to 0.05 for the 22%-doped film. One report shows that part of the Pb atoms in Bi_2Te_3 are electrically inactive, forming a seven-layer lamellae of Te–Bi–Te–Pb–Te–Bi–Te (septuple layer, SL).²⁷⁾ Furthermore, it has recently been reported in Refs. 28–31 that Pb, Bi, and Te can be used to fabricate other topological insulator materials such as PbBi_2Te_4 , PbBi_4Te_7 , and $\text{PbBi}_6\text{Te}_{10}$. These materials are formed by repeating not only QLs, but a combination of QLs and SLs. Thus, it can be concluded that Pb-alloying does not only affect the carrier density of Bi_2Te_3 , but may also be changing the crystal structure itself. Figure 6 shows the RHEED oscillation during film growth. After the completion of a wetting layer (0), QL-by-QL growth occurs for the undoped film. We note that the interval between the first peak (1) and the second peak (2) decreases with increasing Pb concentration. For the 16.7%-doped film, the ratio of the time it takes for the first, second, and third peak

structure (peak1–peak0 : peak2–peak1 : peak3–peak2) $\sim 7 : 3 : 7$. This suggests the formation of a SL–QL–SL structure, and hence, a PbBi_4Te_7 film. This can also be seen from the change in the shape of the Dirac cone. Figure 7 shows the constant energy contour (CEC) mapping at the DP. While the CEC for the pristine film has a rather large and fuzzy circular feature around the $\bar{\Gamma}$ point owing to the overlap with the bulk valence band, this circle shrinks as the Pb concentration increases. Once the bulk conduction band exceeds E_F , the CEC at the DP becomes a “real point” [Figs. 7(e) and 7(f)], implying that the overlap between the surface states and bulk valence band has been eliminated and the Dirac cone has become isolated. While a precise description of the structure would require further investigation, it is clear that Pb-doped Bi_2Te_3 films have an ideal, well-isolated Dirac cone in contrast to the undoped Bi_2Te_3 shown in Fig. 2.

In summary, we found that it is possible to fabricate a truly bulk insulating Bi_2Te_3 film by $\sim 10\%$ Pb incorporation during film growth at $T_{Si} = 350 \text{ K}$. The Dirac cone becomes well isolated from the bulk states and is more ideal than that of the pristine Bi_2Te_3 . The measured film conductivity is consistent with the change in Fermi level revealed by ARPES.

3.3 Pb doping dependence: high T_{Si}

Let us discuss the effect of Pb doping when the films were fabricated at a high substrate temperature ($T_{Si} = 449 \text{ K}$). Figure 8 shows the evolution of the Fermi surface (top row) and the band dispersion (bottom row) for 3 QL Bi_2Te_3 films with a Pb doping concentration of 0 (a), 2.5 (b), 4.4 (c), 10.0 (d), 15.2 (e), and 20.3% (f) (only the band dispersion). The red line indicates the position of the DP. We can see that the size of the Fermi surface changes only slightly. Since the intensity at the center of the Fermi surface remains, the bulk conduction band crosses the Fermi level for all Pb concentrations, although the distinction between the surface and bulk states is extremely difficult to see. Thus, it is not possible to estimate the respective carrier densities. The DP seems to shift slightly towards E_F for the 2.5 (b) and 4.4% (c) doped samples, but moves away from E_F to higher binding energy for the 10.0–20.3% samples in (d)–(f). Furthermore, the shape of the Dirac cone appears to change as Pb is incorporated. The velocity (slope) becomes smaller as Pb is increased. This suggests the formation of another topological insulator material made up of Pb, Bi, and Te. To investigate this effect, we have examined the RHEED intensity oscillation. The results are shown in Fig. 6. Since

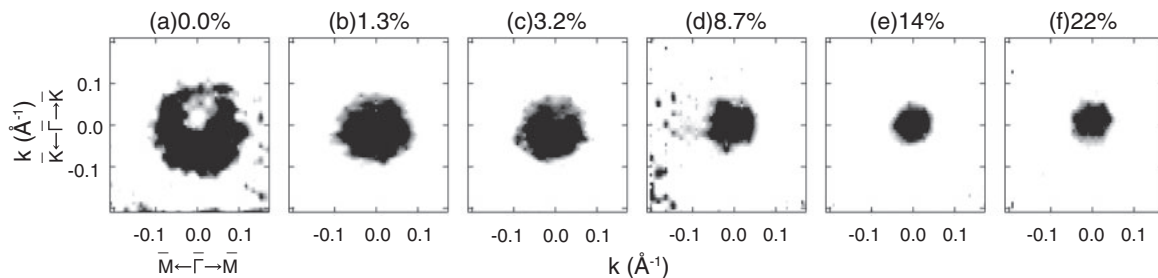


Fig. 7. Constant energy contour mapping at the Dirac point energy for 3 QL Bi_2Te_3 films with varying Pb doping concentration.

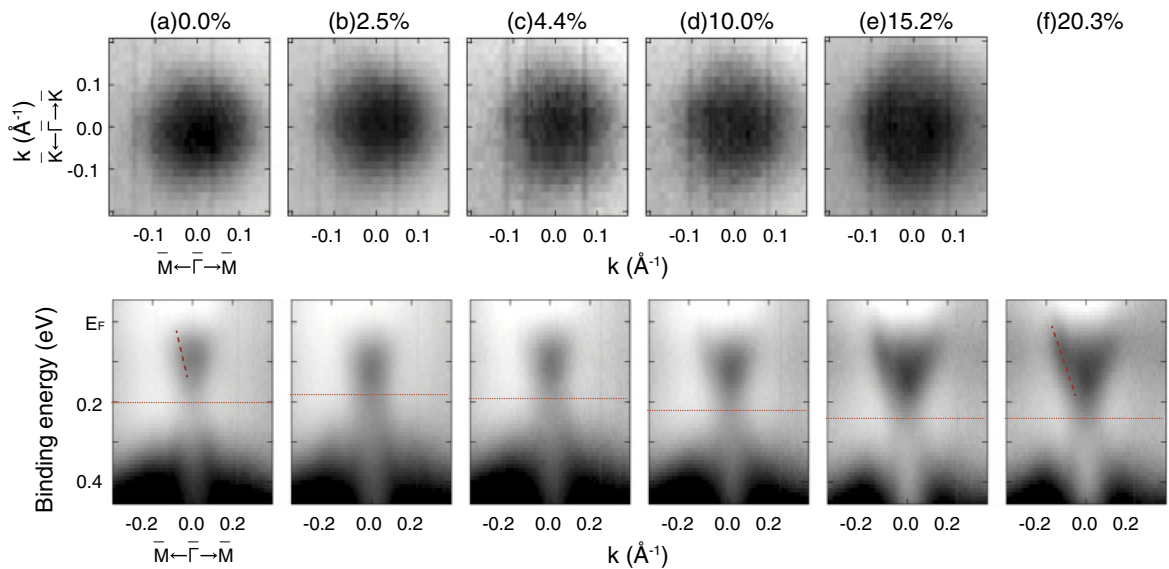


Fig. 8. (Color online) Fermi surface (top row) and band dispersion (bottom row) for 3 QL Bi_2Te_3 films with a Pb doping concentration of 0 (a), 2.5 (b), 4.4 (c), 10.0 (d), 15.2 (e), and 20.3% (f) (only the band dispersion). The red line indicates the position of the Dirac point. The distinction between the bulk and surface states is not clear for these films, but the dashed lines near E_F in (a) and (f) illustrate the dispersion of the Dirac cone.

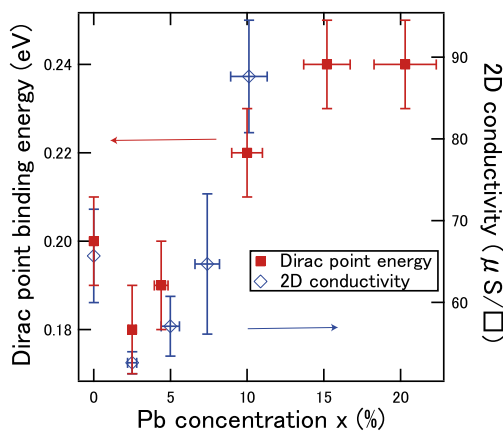


Fig. 9. (Color online) Variation of the Dirac point position (from Fig. 8) with the measured film 2D conductivity.

the growth mode at high substrate temperature is of a step-flow type,²⁵⁾ we could not observe any oscillatory behavior, and it was difficult to determine which alloy was formed. The question of how the difference in T_{Si} influences the Fermi-level tuning of Bi_2Te_3 films as well as the actual structure of the Pb-doped films remain unclear. Further measurements are needed to determine the real atomic structure of the films shown in Figs. 8(d)–8(f).

Figure 9 compares the measured film conductivity (blue open diamonds) and the shift in the DP (red filled squares). It can be seen that the two follow the same trend: A slight drop is observed at the low-concentration Pb doping, then both start to increase with further Pb incorporation. This suggests that the conductivity is basically determined by the carrier density, which was also discussed in the previous section. However, since these films are not bulk insulating films, the absolute values of the conductivity shown in Fig. 9 are higher than $20 \mu\text{S}$ (Fig. 5), which is the value measured for the film that the bulk band does not cross E_F [Figs. 4(e) and 4(f)].

To summarize, we have found that it is not possible to fabricate a truly bulk insulating Bi_2Te_3 film by Pb incorporation during film growth at $T_{\text{Si}} = 450 \text{ K}$, although there is some shift. It is likely that a different structure composed of Pb, Bi, and Te is formed, judging by the change in the shape of the Dirac cone.

4. Summary

In conclusion, we tried to tune the Fermi level of a 3 QL Bi_2Te_3 film to realize a bulk insulating material using one of two methods. The first method, which involved changing the Si substrate temperature during film deposition (350–449 K), had some effect in reducing the bulk residual carriers. However, we could not fabricate a film in which only the surface-state bands crossed the Fermi level. The second method was to incorporate Pb during film growth by co-deposition of Bi, Pb, and Te with controlled ratios of deposition rates. When the films were grown at a relatively low substrate temperature, we observed a systematic shift in the Fermi level and obtained a bulk insulating film. The measured film conductivity was consistent with the change in DP position. These films can hopefully be utilized in electronic device applications. For the films grown at a high substrate temperature, the Fermi level could be changed slightly, but only a bulk n-type film was obtained. Pb incorporation changed the shape of the Dirac cone, which likely suggests the formation of a stoichiometric ternary alloy of Bi, Pb, and Te.

Acknowledgments

This work was supported by Grants-in-Aid from the Japan Society for the Promotion of Science (Nos. 22656011 and 23686007), the JGC-S Scholarship Foundation, the Kao Foundation for Arts and Sciences, and the Support Center for Advanced Telecommunications Technology Research. The ARPES experiments were performed under the UVSOR Proposal Nos. 22-521, 23-515, and 24-521.

- 1) C. L. Kane and E. J. Mele: *Phys. Rev. Lett.* **95** (2005) 146802.
- 2) D. Hsieh, Y. Xia, D. Qian, L. Wray, J. H. Dil, F. Meier, J. Osterwalder, L. Patthey, J. G. Checkelsky, N. P. Ong, A. V. Fedorov, H. Lin, A. Bansil, D. Grauer, Y. S. Hor, R. J. Cava, and M. Z. Hasan: *Nature* **460** (2009) 1101.
- 3) A. Nishide, A. A. Taskin, Y. Takeichi, T. Okuda, A. Kakizaki, T. Hirahara, K. Nakatsuji, F. Komori, Y. Ando, and I. Matsuda: *Phys. Rev. B* **81** (2010) 041309(R).
- 4) K. Miyamoto, A. Kimura, T. Okuda, H. Miyahara, K. Kuroda, H. Namatame, M. Taniguchi, S. V. Ereemeev, T. V. Menshchikova, E. V. Chulkov, K. Kokh, and O. Tereshchenko: *Phys. Rev. Lett.* **109** (2012) 166802.
- 5) S. Souma, M. Komatsu, M. Nomura, T. Sato, A. Takayama, T. Takahashi, K. Eto, K. Segawa, and Y. Ando: *Phys. Rev. Lett.* **109** (2012) 186804.
- 6) T. Misawa, T. Yokoyama, and S. Murakami: *Phys. Rev. B* **84** (2011) 165407.
- 7) R. Yu, W. Zhang, H. J. Zhang, S. C. Zhang, X. Dai, and Z. Fang: *Science* **329** (2010) 61.
- 8) L. Fu and C. L. Kane: *Phys. Rev. Lett.* **100** (2008) 096407.
- 9) C. W. J. Beenakker: *Annu. Rev. Condens. Matter Phys.* **4** (2013) 113.
- 10) O. A. Tretiakov, Ar. Abanov, and J. Sinova: *Appl. Phys. Lett.* **99** (2011) 113110.
- 11) Y. L. Chen, J. G. Analytis, J.-H. Chu, Z. K. Liu, S.-K. Mo, X. L. Qi, H. J. Zhang, D. H. Lu, X. Dai, Z. Fang, S. C. Zhang, I. R. Fisher, Z. Hussain, and Z.-X. Shen: *Science* **325** (2009) 178.
- 12) Y. S. Hor, J. G. Checkelsky, D. Qu, N. P. Ong, and R. J. Cava: [arXiv:1006.0317](https://arxiv.org/abs/1006.0317).
- 13) A. A. Taskin, Z. Ren, S. Sasaki, K. Segawa, and Y. Ando: *Phys. Rev. Lett.* **107** (2011) 016801.
- 14) Z. Ren, A. A. Taskin, S. Sasaki, K. Segawa, and Y. Ando: *Phys. Rev. B* **85** (2012) 155301.
- 15) H. Bando, K. Koizumi, Y. Oikawa, K. Daikohara, V. A. Kulbachinskii, and H. Ozaki: *J. Phys.: Condens. Matter* **12** (2000) 5607.
- 16) J. G. Analytis, R. D. McDonald, S. C. Riggs, J. Chu, G. S. Boebinger, and I. R. Fisher: *Nat. Phys.* **6** (2010) 960.
- 17) T. Tanikawa, I. Matsuda, R. Hobar, and S. Hasegawa: *e-J. Surf. Sci. Nanotechnol.* **1** (2003) 50.
- 18) M. Yamada, T. Hirahara, R. Hobar, S. Hasegawa, H. Mizuno, Y. Miyatake, and T. Nagamura: *e-J. Surf. Sci. Nanotechnol.* **10** (2012) 400.
- 19) Y. Sakamoto, T. Hirahara, H. Miyazaki, S. Kimura, and S. Hasegawa: *Phys. Rev. B* **81** (2010) 165432.
- 20) Y.-Y. Li, G. Wang, X.-G. Zhu, M.-H. Liu, C. Ye, X. Chen, Y.-Y. Wang, K. He, L.-L. Wang, X.-C. Ma, H.-J. Zhang, X. Dai, Z. Fang, X.-C. Xie, Y. Liu, X.-L. Qi, J.-F. Jia, S.-C. Zhang, and Q.-K. Xue: *Adv. Mater.* **22** (2010) 4002.
- 21) T. Zhang, P. Cheng, X. Chen, J. Jia, X. Ma, K. He, L. Wang, H. Zhang, X. Dai, Z. Fang, X. Xie, and Q. Xue: *Phys. Rev. Lett.* **103** (2009) 266803.
- 22) T. Hirahara, G. Bihlmayer, Y. Sakamoto, M. Yamada, H. Miyazaki, S.-I. Kimura, S. Blügel, and S. Hasegawa: *Phys. Rev. Lett.* **107** (2011) 166801.
- 23) M. D'angelo, K. Takase, N. Miyata, T. Hirahara, S. Hasegawa, A. Nishide, M. Ogawa, and I. Matsuda: *Phys. Rev. B* **79** (2009) 035318.
- 24) K. Park, J. Heremans, V. Scarola, and D. Minic: *Phys. Rev. Lett.* **105** (2010) 186801.
- 25) G. Wang, X. Zhu, Y. Sun, Y. Li, T. Zhang, J. Wen, X. Chen, K. He, L. Wang, X. Ma, J. Jia, S. B. Zhang, and Q. Xue: *Adv. Mater.* **23** (2011) 2929.
- 26) We should note that the substrate temperature shown in the present study is lower than that reported in Ref. 25. This is probably due to the difference in the estimation. In Ref. 25, it is most likely that an optical pyrometer is used. However, since we did not have such instrument to measure low temperature, we extrapolated the current-temperature curve obtained for the data points above 800 K. In this estimation, 350–450 K was the only temperature range that we could fabricate a Bi₂Te₃ thin film.
- 27) T. Plecháček, P. Lošťák, J. Navrátil, and T. Černohorský: *Cryst. Res. Technol.* **33** (1998) 911.
- 28) H. Jin, J.-H. Song, A. J. Freeman, and M. G. Kanatzidis: *Phys. Rev. B* **83** (2011) 041202.
- 29) S. V. Ereemeev, G. Landolt, T. V. Menshchikova, B. Slomski, Y. M. Koroteev, Z. S. Aliev, M. B. Babanly, J. Henk, A. Ernst, L. Patthey, A. Eich, A. A. Khajetoorians, J. Hagemeyer, O. Pietzsch, J. Wiebe, R. Wiesendanger, P. M. Echenique, S. T. Tsirkin, I. R. Amiraslanov, J. H. Dil, and E. V. Chulkov: *Nat. Commun.* **3** (2012) 635.
- 30) S. Souma, K. Eto, M. Nomura, K. Nakayama, T. Sato, T. Takahashi, K. Segawa, and Y. Ando: *Phys. Rev. Lett.* **108** (2012) 116801.
- 31) K. Kuroda, H. Miyahara, M. Ye, S. V. Ereemeev, Yu. M. Koroteev, E. E. Krasovskii, E. V. Chulkov, S. Hiramoto, C. Moriyoshi, Y. Kuroiwa, K. Miyamoto, T. Okuda, M. Arita, K. Shimada, H. Namatame, M. Taniguchi, Y. Ueda, and A. Kimura: *Phys. Rev. Lett.* **108** (2012) 206803.



Masaki Aitani received his master's degree in physics from University of Tokyo in 2013. He is currently working at Fujitsu Limited.



Manabu Yamada received his master's degree in physics from the University of Tokyo in 2012. He is currently working at Toshiba Corporation.



Yusuke Sakamoto received his master's degree in physics from University of Tokyo in 2011. He is currently working at Mitsubishi Electric Corporation.



Hidetoshi Miyazaki received his Ph. D. degree in Engineering from Nagoya University in 2009. From 2009 to 2011, he worked at the UVSOR Facility, Institute for Molecular Science, as a Postdoctoral Fellow. Since 2011, he has been working at the Center for Fostering Young and Innovative Researchers, Nagoya Institute of Technology, as an Assistant Professor.



Toru Hirahara obtained his Ph. D. degree in science from the department of physics, University of Tokyo in 2008. Since 2007, he is an assistant professor at the department of physics, University of Tokyo. His major interest is experimental surface physics, especially exploring novel spin-orbit coupling effects at nonmagnetic surfaces.



Masaharu Matsunami received Ph. D. degree in Physics from Kobe University in 2004. From 2004 to 2007, he worked at RIKEN SPring-8 Center as a Special Postdoctoral Researcher. From 2007 to 2010, he worked at the Institute for Solid State Physics (ISSP), the University of Tokyo, as a Postdoctoral Fellow of the Japan Society for the Promotion of Science (JSPS). Since 2010, he has worked at UVSOR Facility in the Institute for Molecular Science, as an Assistant Professor.



Shin-ichi Kimura was born in Fukushima Prefecture, Japan in 1966. He obtained his B. Sc. (1988), M. Sc. (1990), and D. Sc. (1991) degrees from Tohoku University. He was a postdoctoral fellow at JSPS (1991–1993), a research associate at Kobe University (1993) and at Institute for Molecular Science (1993–1998), and an associate professor at Kobe University (1998–2002) and at Institute for Molecular Science (2002–2013). Since 2013, he has been a professor at Osaka University.

He has worked on studies of electronic structure of correlated materials by an infrared/terahertz spectroscopy and an angle-resolved photoemission spectroscopy and synchrotron radiation instrumentations. His research is also now focused on the investigation of electronic structure of solids and soft-matters at multi-extreme conditions.



Shuji Hasegawa obtained the master's degree in science from the department of physics, University of Tokyo in 1985. He has worked in the Advanced Research Laboratory, Hitachi, Ltd. from 1985 to 1990, and since 1990 he has been an assistant/associate/full professor at the department of physics, University of Tokyo. His major interest is experimental surface physics, including surface transport, microscopy, spectroscopy, and diffraction.